Supervised Learning meets Active Noise Control: a Modeling Approach to Feedforward Disturbance Rejection

Ilja Faktorovich[1] and Christian Bohn[2]

Abstract— **This paper presents an approach for feedforward disturbance rejection for open or closed loop controlled plants combining the Machine Learning (ML) perspective on supervised learning with basic paradigms of the active noise cancelling (ANC) framework. In contrast to a broad amount of the proposed methodology in this area, neither a linear primary path nor a time invariant secondary path are assumed. Moreover, the disturbance source has a multi-channel structure, increasing complexity to the considered setup. The proposed methodology applies a Neural Network (NN) based feedforward controller which can be optimized iteratively or in closed form depending on the network structure. A two-staged approach is presented, transforming the control problem into a supervised learning setting and applying well-known methods of system identification and Machine Learning. This simple but effective procedure bridges the gap between supervised learning and ANC methods and highlights new fields of application for the subsequent combined approach. An experimental evaluation on the Air-Fuel-Ratio (AFR) control of a spark ignited engine is provided to demonstrate the practicability and effectiveness of the proposed methodology.**

I. INTRODUCTION

The interdisciplinary field of ANC combines insights from Control Theory, System Identification and Signal Processing for almost a whole century with the objective to attenuate unwanted noise in a measurable signal. Despite its rich methodological and algorithmical foundation the applications of ANC are nearly exclusively in the area of acoustics and vibration. However, even in this area the amount of industrial applications of ANC approaches is limited [1]. On the other hand, a vast majority of industrial control applications involve PID controllers with or without an additional feedforward control [2]. If the disturbance source is measurable, a feedforward controller can be tuned to attenuate the effect on the plant. This process typically requires the plant and disturbance models to be linear time invariant (LTI) and involves the inversion of the plant model and an estimate of the disturbance transfer function to compute the transfer function of the corresponding feedforward controller [3], [4]. Since this direct approach may lead to an unstable or non-causal feedforward controller, several procedures have been proposed to circumvent this problem. In this context a major class of feedforward tuning schemes pose restrictive assumptions on the controlled system and the disturbance model. This creates the opportunity to reduce the feedforward controller to a static gain or a lead-lag filter and to provide tuning rules for practical implementation [5], [6]. Data driven feedforward control design is a recent alternative to the aforementioned methodology e.g. using Iterative Learning Control, Reinforcement Learning or fuzzyfication [7], [8], [9]. Other attempts in feedforward control design utilize the well-known filtered-x least mean square (FxLMS) algorithm from the ANC framework e.g. for tracking and disturbance attenuation [10], [11]. When considering nonlinear disturbances with a variety of dynamic components and a set of a priori unknown disturbance source signals the estimation of the disturbance model itself can be a challenging task. A similar problem arises in nonlinear multiband ANC systems where an adaptive finite impulse response (FIR) filter is not suitable to account for nonlinearities in the primary path. For this reason, more recent approaches utilize NNs as a feedforward compensator [12] and formulate ANC as a supervised learning problem in the special case of a spectral mapping setup without modeling the secondary path explicitly. The contribution of the present work is to provide a universal approach to designing feedforward disturbance rejection for multidimensional nonlinear disturbances acting either on the system input or output of a SISO system. Thereby, the proposed methodology is capable of dealing with a linear parameter varying (LPV) plant and solves the control problem offline. For this purpose, the close connection between ANC and disturbance rejection feedforward control is exploited and transferred in a supervised learning problem. The data for the presented approach can either be generated from an open or closed loop for systems that cannot be operated without an additional feedback controller. In order to handle possible nonlinear disturbance effects widespread nonlinear ML models can be introduced to represent the feedforward compensator. The approach is demonstrated on the AFR control of an spark ignited gasoline engine by transforming a disturbance rejection problem into a modeling task and solving it offline using data collected from the system. The remainder of this paper is organized as follows. First, in Section II the control problems of interest are introduced and the close connection to ANC is pointed out. Section II introduces the proposed approach where the open loop and closed loop scenarios are treated in subsection A and subsection B respectively. Finally, the implementation example is shown in Section III where the proposed methodology is evaluated on a spark ignited combustion engine with some concluding remarks in Section IV.

This work was supported in part by the Volkswagen AG.

[1]I. Faktorovich is with the Volkswagen AG, Berliner Ring 2, 38440 Wolfsburg, Germany. (phone: +49-5361-986958; e-mail: ilja.faktorovich@volkswagen.de).

[2]C. Bohn is with the Clausthal University of Technology, Leibnizstraße 28, 38678 Clausthal-Zellerfeld, Germany. (phone: +49-5323-723129; e-mail: bohn@iei.tu-clausthal.de).

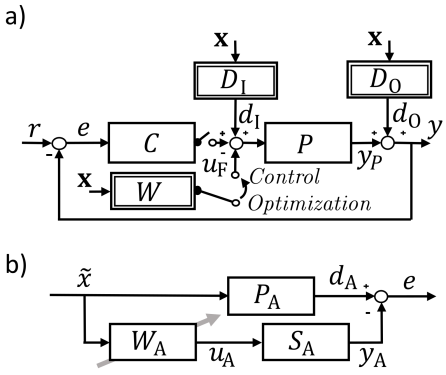

Fig. 1. Block Diagrams of feedforward control problems a) Feedforward disturbance rejection in open loop – input and output disturbance case. Two-stage approach of offline optimization and deployment b) Single channel ANC adaptive feedforward control.

II. Feedforward Disturbance Rejection

The following discrete time disturbance rejection control problems can be formalized according to the block diagram in Fig. 1 a). It is assumed here that the disturbance affects the system input or system output, respectively. The operators D_I and D_O represent general nonlinear systems where $\mathbf{x}$ is the disturbance source vector and d_O and d_I the output and input disturbance respectively. It is assumed that the system P is optionally operated by a feedback controller C in closed loop where y_p denotes the system output and y the measurement variable. The closed loop and open loop cases are treated separately in the following. The controller W is to be tuned to generate a control action u_F to reduce some signal norm of the control error e. Here, for simplicity, setpoint r shall be zero. In Fig. 1b) P_A and S_A are transfer functions of the primary and secondary path and $\tilde{x}$ is the single channel noise source. The filter W_A is tuned to generate the signal u_A to cancel the disturbance d_A using the secondary path output y_A. It should be pointed out that the control loop in Fig. 1a) when operated in open loop and subject to an output disturbance only is equivalent to the standard ANC Problem in Fig. 1b). However, for the ANC case in in Fig. 1b) the transfer functions are typically assumed to be LTI and some variant of the FxLMS is used to tune the Filter W_A. When applying this kind of ANC approach to the open loop control problem in Fig. 1a) P needs to obey LTI properties. In the following P is only assumed to be LPV extending the approach to feedforward controllers to a larger set of systems. Furthermore, similar to a prior estimated secondary path in ANC an estimate of the varying impulse response $p_i[\rho[k]]$ of P with the known scheduling variable $\rho[k]$ is assumed to be known. For the output disturbance case in 1a) the solution

$$W[z] = \frac{D_\mathrm{O}[z]}{P[z]} \tag{1}$$

can be considered optimal if D_O and P are LTI. However, since Eq. (1) can lead to a non-causal or unstable controller, traditional feedforward control design deals with this inversion problem e.g. by utilizing model matching or approximation techniques [4]. A similar feedforward control design procedure can be applied for the ANC problem in 1b) however, it is usually solved by adapting a filter W_A online. Let P_A be approximated by an FIR filter

$$\hat{P}_\mathrm{A}[z] = p_0 + p_1 z^{-1} + ... + p_c z^{-c} \tag{2}$$

and the feedforward controller W_A by

$$W_\mathrm{A}[z] = w_\mathrm{o} + w_\mathrm{1} z^{-1} + ... + w_m z^{-m} \tag{3}$$

of the order c and m respectively. The adaptation of the Filter W_A is then performed online by introducing a cost function

$$J_\mathrm{A}[n] = \frac{1}{2}e^2[n] = \frac{1}{2}(d_\mathrm{A}[n] - \sum_{i=0}^{c} p_i[n]\tilde{\mathbf{x}}^\mathrm{T}[n-i]\mathbf{w}[n-i])^2 \tag{4}$$

where $\mathbf{w}[n] = [w_0[n], ...w_m[n]]^\mathrm{T}$ is the parameter vector and $\tilde{\mathbf{x}}[n] = [\tilde{x}[n], ..., \tilde{x}[n-m]]^\mathrm{T}$ are the stacked elements of the disturbance source signal. The partial derivative of Eq. (4) w.r.t. the controller parameter vector is given by

$$\frac{\partial J_\mathrm{A}[n]}{\partial \mathbf{w}^\mathrm{T}} = e[n](\sum_{i=\mathrm{o}}^{c} p_i[n]\tilde{\mathbf{x}}[n-i]) \tag{5}$$

and used in a gradient descent fashion for the online parameter update in FxLMS style algorithms [13]. Online implementation allows the controller to handle a time-varying primary path P_A which is the common objective in ANC. The cost function in Eq. (4) is similar to the formulation of a system identification or supervised learning task. Since the proposed approach is not designed to track time-varying disturbance operators D_I and D_O for the task in Fig. 1a) we will focus on an offline solution from collected data. Specifically, the data sets

$$\mathcal{X} = \{\mathbf{x}[i] \in \mathbb{R}^\mathrm{l}, \mid i = 1, 2, \ldots, N\} \tag{6}$$

$$\mathcal{Y} = \{y[i] \mid i = 1, 2, \ldots, N\} \tag{7}$$

$$\mathcal{P} = \{\rho[i] \mid i = 1, 2, \ldots, N\} \tag{8}$$

need to be collected from the open-loop operated system in Fig. 1a). In case the plant P has to be operated in a closed loop the feedback controller output

$$\mathcal{U}_c = \{u_c[i] \mid i = 1, 2, \ldots, N\} \tag{9}$$

needs to be stored additionally. In the next subsection the open loop case with the corresponding optimization problem formulation is introduced. It is straightforward to set up a similar optimization criterion to Eq. (4) by exploiting the linearity of the LPV controlled plant P and optimize for the structure and parameters of $W(.)$ to deal with possible highly nonlinear disturbance system dynamics.

A. Open loop feedforward control optimization

As established in the previous section the optimization procedure for the feedforward controller is performed using data collected from the plant. Let the control law

$$u_\mathrm{F}[n] = \boldsymbol{\phi}^\mathrm{T}(\bar{\mathbf{x}}[n])\mathbf{w} \tag{10}$$

be a linear parametric transformation of the augmented control input vector

$$\bar{\mathbf{x}}[k] = [\mathbf{x}^{\mathrm{T}}[k], \rho[k]]^{\mathrm{T}} \tag{11}$$

with a basis function $\boldsymbol{\phi} : \mathbb{R}^{\mathrm{l}+1} \rightarrow \mathbb{R}^{\mathrm{m}}$, since for an LPV plant the control actions generally depend on the scheduling variable. Similar to Eq. (4) the cost function for the feedforward control problem in Fig. 1a) can be stated as

$$J_F = \frac{1}{2} \sum_{n=1+c}^{N} \left(y[n] - \sum_{i=0}^{c} \hat{p}_i[\rho[n]] \boldsymbol{\phi}^{\mathrm{T}}(\bar{\mathbf{x}}[n-i])\mathbf{w} \right)^2 \tag{12}$$

where $\hat{p}_i[\rho[n]]$ is the FIR estimate of the time-varying impulse response of the plant of length $c+1$. Without loss of generalization setpoint r is assumed to be zero. By introducing the matrices

$$\hat{\mathbf{P}} = \begin{bmatrix} \hat{p}_0[\rho[1]] & 0 & ... & ... & 0 \\ \hat{p}_1[\rho[2]] & \hat{p}_0[\rho[2]] & 0 & ... & 0 \\ ... & ... & ... & ... & 0 \\ \hat{p}_c[\rho[c]] & \hat{p}_{c-1}[\rho[c]] & ... & ... & 0 \\ 0 & \hat{p}_c[\rho[c+1]] & ... & ... & 0 \\ 0 & 0 & ... & ... & ... \\ ... & ... & ... & \hat{p}_0[\rho[N-1]] & 0 \\ 0 & 0 & ... & \hat{p}_1[\rho[N]] & \hat{p}_0[\rho[N]] \end{bmatrix} \tag{13}$$

$$\boldsymbol{\Phi} = \begin{bmatrix} \boldsymbol{\phi}(\bar{\mathbf{x}}[1]) \\ ... \\ \boldsymbol{\phi}(\bar{\mathbf{x}}[N]) \end{bmatrix} \tag{14}$$

as well as the measured output vector $\mathbf{y} = [y[1], ..., y[n]]^{\mathrm{T}}$ the cost function from Eq. (12) can be stated in matrix vector form including a matrix representation of the LPV system. The closed form solution of the resulting cost function

$$J_F = \frac{1}{2}(\mathbf{y} - \hat{\mathbf{P}}\boldsymbol{\Phi}\mathbf{w})^{\mathrm{T}}(\mathbf{y} - \hat{\mathbf{P}}\boldsymbol{\Phi}\mathbf{w}) \tag{15}$$

is then formulated by incorporating the necessary and sufficient condition $\frac{\partial J_F}{\partial \mathbf{w}^{\mathrm{T}}} = 0$. The closed form solution for the parameter vector

$$\mathbf{w}^* = (\boldsymbol{\Phi}^{\mathrm{T}}\hat{\mathbf{P}}^{\mathrm{T}}\hat{\mathbf{P}}\boldsymbol{\Phi})^{-1}\boldsymbol{\Phi}^{\mathrm{T}}\hat{\mathbf{P}}^{\mathrm{T}}\mathbf{y} \tag{16}$$

is closely related to a least squares parameter estimation problem extended by the estimate of the system transform matrix $\hat{\mathbf{P}}$. By inspection of Eq. (4) and Eq. (12) the parameter vector in Eq. (16) provides an optimal solution in a least-squares sense. Since the system is operated in an open loop the system output is solely driven by the disturbance so that $\mathbf{y}$ and a vector of stacked output disturbances $\mathbf{d}_A$ can be considered interchangeably in an output disturbance case. However, if the controlled system is subject to an input disturbance $d_{\mathrm{I}}[n] = \boldsymbol{\phi}_{\mathrm{I}}(\mathbf{x}[n])\mathbf{w}_{\mathrm{I}}$ with some arbitrary $\mathbf{w}_{\mathrm{I}}$ and $\boldsymbol{\phi}_{\mathrm{I}}$, then

$$\mathbf{y} = \mathbf{P}\boldsymbol{\Phi}_{\mathrm{I}}\mathbf{w}_{\mathrm{I}} \tag{17}$$

holds for the measured vector $\mathbf{y}$ where $\mathbf{P}$ is the system transform matrix and $\boldsymbol{\Phi}_{\mathrm{I}}$ the basis function of the disturbance analogously to Eq. (14). Substitution of Eq. (17) in Eq. (13) yields

$$\mathbf{w}^* = (\boldsymbol{\Phi}^{\mathrm{T}}\hat{\mathbf{P}}^{\mathrm{T}}\hat{\mathbf{P}}\boldsymbol{\Phi})^{-1}\boldsymbol{\Phi}^{\mathrm{T}}\hat{\mathbf{P}}^{\mathrm{T}}\mathbf{P}\boldsymbol{\Phi}_{\mathrm{I}}\mathbf{w}_{\mathrm{I}} \tag{18}$$

where $\mathbf{w}^* \approx \mathbf{w}_{\mathrm{I}}$ when $\hat{\mathbf{P}}$ is a sufficiently accurate estimate for $\mathbf{P}$ and $\boldsymbol{\Phi}$ is chosen correctly. The activation of the feedforward controller in the second step of the procedure involves a change of sign as shown in Fig. 1a). This leads to a superposition of the control and the disturbance acting on the system output leading to an optimal disturbance cancellation in a least squares error sense. The plant transfer function can be subject of a high relative degree or a process dead time which reduces the rank of $\mathbf{P}$ and limits the general achievable disturbance rejection performance for an output disturbance case. However, the proposed offline feedforward design procedure creates the opportunity to estimate the performance of the feedforward controller prior to its final application by observing the objective in Eq. (15) while considering different model structure and parameter sets. Therefore, the objective function of the control parameters is interpreted as a regression task or a supervised learning problem. Generally the control law can be non linear-parametric and the objective in Eq. (15) can be optimized using any suitable approach, which is also exemplified in the application example. The next subsection extends the proposed approach to a plant that has to be operated by a feedback controller during the data collection phase.

B. Closed loop feedforward control optimization

In contrast to a plant P operated in an open loop it is not possible to directly measure the impact of the disturbance on the plant output in a closed loop. For a linear system the output y can be understood as a superposition of the system output driven by the feedback controller and the disturbance. Since the feedback control actions u_c are assumed to be known it is possible to use the estimate $\hat{p}_i[\rho[n]]$ to isolate the disturbance impact on y. The block diagram in Fig. 2 provides an illustration of the procedure. The cost function of Eq. 15 has then to be modified resulting in

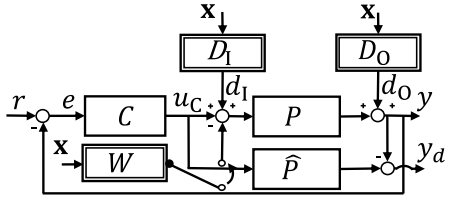

Fig. 2. Block Diagrams of disturbance isolation in a closed loop controlled plant.

$$J_{Fc} = \frac{1}{2}(\mathbf{y_d} - \hat{\mathbf{P}}\boldsymbol{\Phi}\mathbf{w})^{\mathrm{T}}(\mathbf{y_d} - \hat{\mathbf{P}}\boldsymbol{\Phi}\mathbf{w}) \tag{19}$$

where $\mathbf{y_d} = \mathbf{y} - \hat{\mathbf{P}}\mathbf{u_c}$, $\mathbf{u_c} = [u_c[1], ..., u_c[n]]^{\mathrm{T}}$ and the feedforward control given by Eq. (10). The closed form solution for the parameter vector then yields

$$\mathbf{w}^* = (\boldsymbol{\Phi}^{\mathrm{T}}\hat{\mathbf{P}}^{\mathrm{T}}\hat{\mathbf{P}}\boldsymbol{\Phi})^{-1}\boldsymbol{\Phi}^{\mathrm{T}}\hat{\mathbf{P}}^{\mathrm{T}}\mathbf{y_d} \tag{20}$$

In case an input disturbance of the form Eq. (17) affects the plant the system output $\mathbf{y}$ can be stated as

$$\mathbf{y} = \mathbf{P}\mathbf{\Phi}_{\mathrm{I}}\mathbf{w}_{\mathrm{I}} + \mathbf{P}\mathbf{u}_{\mathbf{c}} \tag{21}$$

and inserted in Eq. (20) resulting in

$$\mathbf{w}^{*} = (\mathbf{\Phi}^{\mathrm{T}}\hat{\mathbf{P}}^{\mathrm{T}}\hat{\mathbf{P}}\mathbf{\Phi})^{-1}\mathbf{\Phi}^{\mathrm{T}}\hat{\mathbf{P}}^{\mathrm{T}}(\mathbf{P}\mathbf{\Phi}_{\mathrm{I}}\mathbf{w}_{\mathrm{I}} + \mathbf{e}_{\mathbf{M}}) \tag{22}$$

for the estimate of the feedforward control parameter vector. Here $\mathbf{e}_{\mathbf{M}} = (\mathbf{P} - \hat{\mathbf{P}})\mathbf{u}_{\mathbf{c}}$ denotes the modeling error of the estimate $\hat{\mathbf{P}}$ of $\mathbf{P}$ under the controller output u_c. In a practical application, we would assume that the estimate of the plant impulse response is subject to some uncertainty so is the plant transform matrix. Comparing Eq. (22) to Eq. (18) reveals that the parameter estimate for the feedforward controller will be generally worse then the same estimate for data that is collected in an open loop and used for an estimate of the form Eq. (16). For this reason it is preferable to estimate the feedforward controller from open loop data when possible. The open loop data feedforward control parameter estimation is subject of the next chapter of the application example also.

III. Experimental Evaluation

For the evaluation of the proposed methodology the AFR control of a gasoline spark ignited (SI) production engine of the EA211evo series is considered. The engine utilizes a direct fuel injection system and has four cylinders with a total displacement of $1498\,\mathrm{cm}^3$. Furthermore, it is equipped with a variable phasing of the intake as well as the outlet camshaft, a variable geometry turbocharger, an intercooler and a wide-band oxygen sensor placed behind the turbine in airflow direction. A schematic of the engine layout is shown in Fig. 3. Due to the event based operation of an internal combustion engine the measurements as well as the control inputs are considered to be subject to the crank angle domain. This leads to a fix sample rate of every $180°$ crank angle and a variable sampling time depending on the engine rotation speed [14]. The signals of interest are measured using the standard series sensor configuration of the engine and recorded using an ETAS ES891.1 connected directly to the engine control unit (ECU). Tab. I provides an overview of the signals of interest. A scaling factor m_c will serve as the control input signal in the following. In order to reduce emissions it is necessary to keep the AFR at a stoichiometric value which is equivalent to $\lambda = 1$. However, since it is not possible to measure the amount of oxygen in the cylinder directly, model based approaches are typically used to estimate the quality and quantity of the in-cylinder air charge. This serves as a foundation to calculate and inject the amount of fuel which would lead to a stoichiometric combustion. From a practical point of view the parameter estimation of a precise dynamical model for the in-cylinder air charge is a very complicated task since an airflow-meter can provide reliable measurements only for steady state engine operation. This can lead to a miscalculation for the calculated fuel mass of the injection process especially during transient engine operation. Additionally, the crank

TABLE I
Signal Nomencalture

n_e	Engine speed (rpm)
m_{in}	Manifold pressure (mbar)
ζ_e	Delta ref. inlet camshaft phase (°)
ζ_a	Delta ref. outlet camshaft phase (°)
t_h	Throttle angle (°)
λ	Air fuel equivalence ratio (1)
m_f	Feedforward control fuel mass (mg/stroke)
m_b	Feedback control output (1)
m_c	Fuel injection factor (1)
e_λ	Lambda deviation - scaled (1)

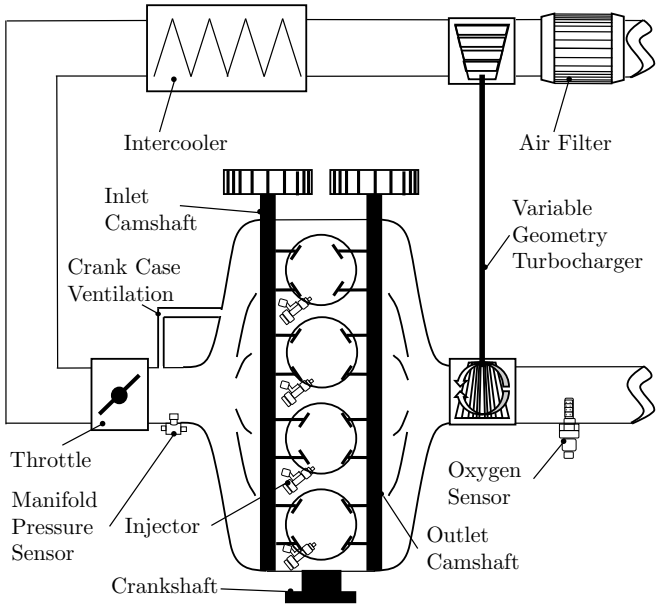

Fig. 3. Schematic of the considered SI engine

case ventilation system allows for hydrocarbon vapors to be part of the combustion and to act as a disturbance on the desired AFR. Other model-based ECU functions e.g. for the calculation of the injected fuel mass can also be subject to modeling errors. All these effects lead to a rich or lean mixture which manifests a non stoichiometric combustion. To comply with privacy requirements, parts of the original AFR measurements are rescaled. The goal for the subsequent control design is to interpret estimation errors or possibly entirely unmodeled effects on the AFR as disturbances and design an appropriate feedforward controller to reduce their impact on the measured λ. Therefore, all the present ECU functions which are part of the calculation of the injected fuel mass are not modified during the control design and evaluation. The block diagram of the AFR control is shown in Fig. 4. The baseline feedforward controller in the software calculates the injected fuel mass m_f. If the feedback controller is active its control variable scales the output of the feedforward controller in order to achieve steady-state reference tracking. For the following investigation the feedback controller is deactivated and an additional NN feedforward controller is designed in order to achieve AFR control enhancement by compensating for unmodelled effects

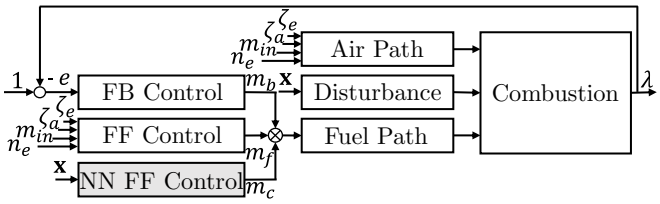

Fig. 4. Abstraction of the AFR control architecture - the feedforward disturbance rejection contoller is highlighted in grey. Here $\mathbf{x}$ is initially unknown and subject to estimation.

and disturbances during transient system operation.

The first step of the control design involves deriving an estimate of the LPV plant impulse response with respect to the system input m_c and the output λ. This LPV impulse response is characterized by the dynamic response of the injector, the oxygen sensor and the transport dead time from the combustion to the oxygen sensor, respectively. The dead time depends on the current volumetric flowrate which itself can be expressed as a function of the crankshaft angular velocity and the volumetric efficiency. Since an event-based sampling is considered, the volumetric efficiency mainly determines the process dead time. As the input and output camshaft positions are set based on the engine rpm and the load, the general expression for the impulse response estimate can be stated

$$\hat{p}_i[\rho[n]] \approx \hat{p}_i[n_e[n], m_{in}[n]] \tag{23}$$

as an approximation. In order to construct an estimate based on Eq. (23) the impulse response for point wise combinations of engine speed and manifold pressure is obtained in the first step. These estimates are then used to construct $\mathbf{P}$ according to Eq. (13) for given trajectories for n_e and m_{in}. An estimate of the impulse response is established for permutations of engine speed in the range from $1500 - 4000$ rpm including six breakpoints and an intake manifold pressure range from $300 - 1100$ mbar with five breakpoints both evenly spaced. For this purpose the test vehicle is placed on a chassis dynamometer where the target engine speed and manifold pressure is set. After an appropriate rest time the feedforward controller output value m_c was used to apply a pseudorandom binary sequence (PRBS) test signal. An illustration of the estimation results is shown in Fig. 5. The dataset for each combination of engine speed and manifold pressure had a total length of 10000 samples where 20% of the data is used for validation and 10% for testing. The total filter length of 51 was estimated using collected data for all operation conditions whereas the plant dead time was estimated for every individual combination of the two independent variables. Additionally, Tikhonov regularization was used to smooth the estimate and enhance cross-validation performance. The coefficient of determination R^2 for the secondary path is in the range of $0.92 - 0.96$ for all estimates. The next step involves the data collection of the system operated under the effect of disturbances. Due to the fact that the system can be operated without the feedback controller for a limited amount of time

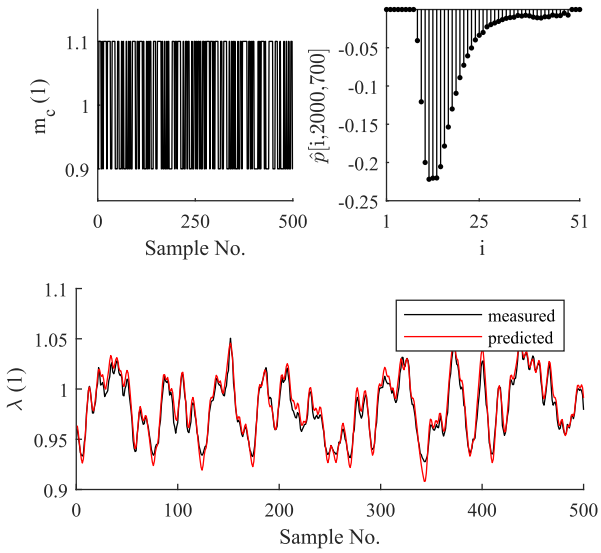

Fig. 5. Illustration of the estimation of FIR Filter coefficients for $n_e = 2000$ rpm and $m_{in} = 700$ mBar. Top Left - Exitation sequence. Top right - filter coefficients. Bottom - cross validation result of system output prediction.

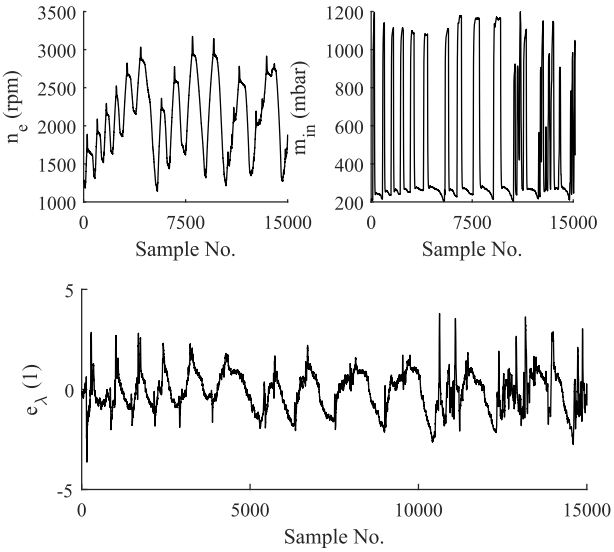

Fig. 6. Engine operation under the influence of disturbances. Lambda deviation scaled.

it will remain deactivated. For the purpose of data collection the vehicle is conditioned to a regular operating temperature of engine oil and coolant and subjected to three urban short drive cycles. Due to the rapid dynamics of the manifold pressure enhancement of feedforward control performance is crucial in this operational range as highlighted in Fig. 6. The rest of the design procedure of the feedforward controller can be treated like a supervised learning problem finding a control structure and features in order to minimize the cost of Eq. (15) where y is replaced by $\lambda - 1$. The rescaled lambda deviation is given by

$$e_\lambda = \frac{\lambda - 1}{\sigma_\lambda} \tag{24}$$

where σ_λ is the standard deviation of λ in the recorded datasets. In this particular example an extreme learning machine (ELM) is used with one layer and 800 neurons using a ReLU activation function where the output layer was optimized using the closed-form solution of Eq. (16). The feature selection for construction of the vector $\mathbf{x}$ was performed using a global optimization based approach. The resulting 80 features are current and different numbers of preceding values of $n_e, m_{in}, \zeta_e, \zeta_a, t_h$ as well as the setpoint of the throttle position. The testing results are presented in Fig. 7 achieving an accuracy of $R^2 \approx 0.87$. The feedforward

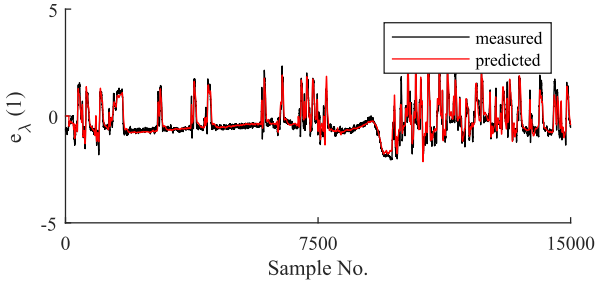

Fig. 7. Feedforward control disturbance effect approximation.

controller is then implemented in the ECU software according to Fig. 4 but the control actions are applied reciprocally with respect to their calculated value in order to attenuate the lumped disturbance effect on λ. Fig. 8 shows the evaluation of the vehicle implementation. Two similar drive cycles were performed with the vehicle to highlight the effectiveness of the proposed approach. Despite the relatively simple structure of the controller the impact of the disturbance can be reduced significantly, enhancing the control performance.

IV. CONCLUSIONS

We presented a new approach for feedforward control design for LTI and LPV systems subjected to measurable nonlinear disturbances. The proposed design procedure transforms the control problem to a supervised learning setting which allows for the use of nonlinear control structures to attenuate disturbance effects. Additionally, the control structure design and feature selection can be evaluated and adjusted in advance to the implementation by offline inspection of the ability of the controller to capture the disturbance dynamics. Implementation results on the AFR control of an SI engine indicate the effectiveness of the proposed methodology.

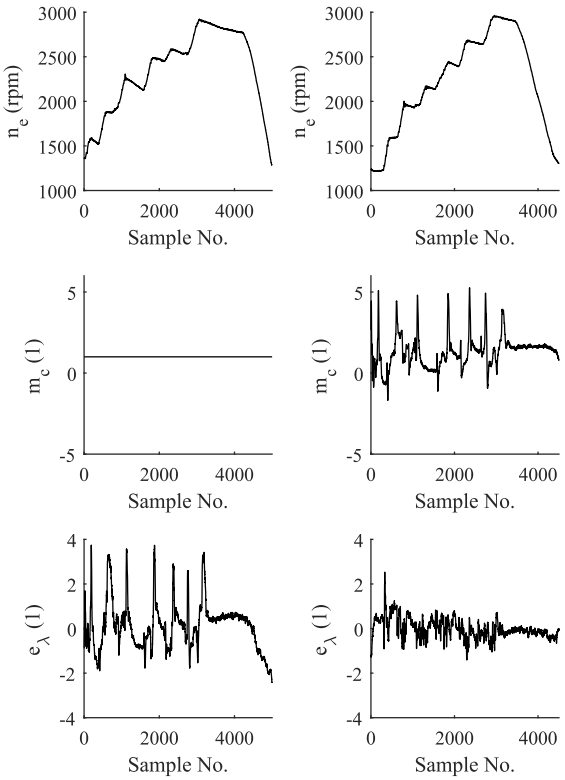

Fig. 8. Vehicle implementation. Left - disabled feedforward control. Right - enabled feedforward control. A reduction of the standard deviation of e_λ by a factor of 2.43 is achieved.

REFERENCES

[1] C. H. Hansen, "Current and future industrial applications of active noise control," *Noise Control Engineering Journal*, vol. 53, no. 5, pp. 181–196, 2005.

[2] M. Jelali, "An overview of control performance assessment technology and industrial applications," *Control engineering practice*, vol. 14, no. 5, pp. 441–466, 2006.

[3] J. L. Guzmán and T. Hägglund, "Simple tuning rules for feedforward compensators," *Journal of Process control*, vol. 21, no. 1, pp. 92–102, 2011.

[4] H. Zhong, L. Pao, and R. de Callafon, "Feedforward control for disturbance rejection: Model matching and other methods," in *2012 24th Chinese Control and Decision Conference (CCDC)*, pp. 3528–3533, IEEE, 2012.

[5] J. L. Guzmán and T. Hägglund, "Tuning rules for feedforward control from measurable disturbances combined with pid control: a review," *International Journal of Control*, vol. 97, no. 1, pp. 2–15, 2024.

[6] M. Hast and T. Hägglund, "Low-order feedforward controllers: Optimal performance and practical considerations," *Journal of Process Control*, vol. 24, no. 9, pp. 1462–1471, 2014.

[7] R. Noack, T. Jeinsch, A. H. A. Sari, and N. Weinhold, "Data-driven self-tuning feedforward control by iterative learning control," in *2014 IEEE 23rd International Symposium on Industrial Electronics (ISIE)*, pp. 2439–2444, IEEE, 2014.

[8] I. Faktorovich, C. Bohn, and J. Vogelsang, "Reinforcement learning motivated feedforward control approach for disturbance rejection and tracking," in *2021 European Control Conference (ECC)*, pp. 138–143, IEEE, 2021.

[9] M. B. Kadri, "Disturbance rejection in nonlinear uncertain systems using feedforward control," *Arabian Journal for Science and Engineering*, vol. 38, pp. 2439–2450, 2013.

[10] N. Wang, K. E. Johnson, and A. D. Wright, "Fx-rls-based feedforward control for lidar-enabled wind turbine load mitigation," *IEEE Transactions on Control Systems Technology*, vol. 20, no. 5, pp. 1212–1222, 2011.

[11] Y. Tang, Z. Zhu, and G. Shen, "Design and experimental evaluation of feedforward controller integrating filtered-x lms algorithm with applications to electro-hydraulic force control systems," *Proceedings of the Institution of Mechanical Engineers, Part C: Journal of Mechanical Engineering Science*, vol. 230, no. 12, pp. 1951–1967, 2016.

[12] H. Zhang and D. Wang, "Deep anc: A deep learning approach to active noise control," *Neural Networks*, vol. 141, pp. 1–10, 2021.

[13] I. T. Ardekani and W. H. Abdulla, "Theoretical convergence analysis of fxlms algorithm," *Signal Processing*, vol. 90, no. 12, pp. 3046–3055, 2010.

[14] C.-F. Chang, N. P. Fekete, A. Amstutz, and J. Powell, "Air-fuel ratio control in spark-ignition engines using estimation theory," *IEEE Transactions on Control Systems Technology*, vol. 3, no. 1, pp. 22–31, 1995.